ACS APPLIED MATERIALS & INTERFACES

RESEARCH ARTICLE

www.acsami.org

Flexible Carbon Nanotube-Based Composite Plates As Efficient Monolithic Counter Electrodes for Dye Solar Cells

Francesco Malara,[†] Michele Manca,[*,‡] Luisa De Marco,[‡] Paola Pareo,[‡] and Giuseppe Gigli[†,‡]

[†]National Nanotechnology Laboratory, CNR Istituto Nanoscienze—Distretto Tecnologico, via per Arnesano 16, 73100 Lecce, Italy

[‡]Center for Biomolecular Nanotechnologies, Italian Institute of Technology, via Barsanti, 73010 Arnesano (Lecce), Italy

ABSTRACT: We demonstrate a general approach to fabricate a novel low-cost, lightweight and flexible nanocomposite foil that can be effectively implemented as a monolithic counter-electrode in dye solar cells. The pivotal aim of this work was to replace not only the platinum catalyzer film, but even the underlying transparent conductive oxide-coated substrate, by means of a monolithic counter electrode based on carbonaceous materials. According to our approach, a proper dispersion of multiwalled carbon nanotubes (MWCNTs) has been added to a dilute polypropylene solution in toluene. The composite solution has been then adequately mixed and subsequently dried by means of a controlled solvent evaporation process; the resulting powder has been modeled by compression molding into thin plates. Four different series of plates have been realized by tuning the carbon nanotubes concentration from 5 wt % to 20 wt %. Finally, a specifically setup reactive ion etching treatment with oxygen plasma has been carried out onto the plate surface to remove the residual polymeric capping layer and allow the embedded CNTs to protrude on top of the surface. A fine-tuning of the morphological features has been made possible by adjusting the plasma etching conditions. For all the treated surfaces, the most meaningful electrochemical parameters have been quantitatively analyzed by means of both electrochemical impedance spectroscopy and cyclic voltammetry measurements. An as high as 13.8 mA/cm^2 photocurrent density, along with a solar conversion efficiency of 6.67%, has been measured for a dye solar cell mounting a counter-electrode based on a 20 wt % CNT nanocomposite.

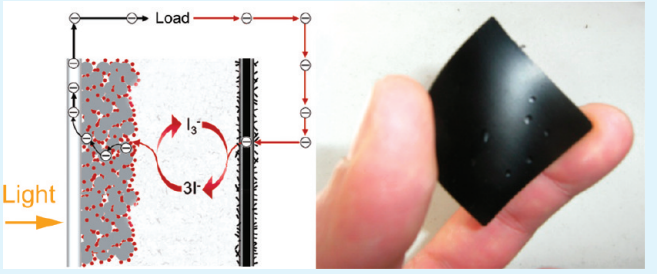

KEYWORDS: dye solar cells, multiwalled carbon nanotubes, counter electrode, electrochemical impedance spectroscopy

1. INTRODUCTION

In 1991 the seminal paper by O'Regan and Grätzel[1] on dye-sensitized solar cells (DSSC) opened up the possibility to the use of devices based on molecular components for the construction of robust large-scale solar electricity production facilities. In this case it was the development of an effective low-cost photovoltaic technology capable to guarantee large flexibility in shape, color, and transparency that outlined the perspective of new commercial opportunities.[2] A dye solar cell consists of a monolayer of photosensitizing dye adsorbed on a mesoporous film of nanocrystalline oxide semiconductor, typically anatase titanium dioxide. Dye molecules are chemisorbed through functional anchoring groups on the surface of the semiconductor, while the pores of the film are generally filled with a iodide/tri-iodide electrolyte. When an incident photon excites the dye, this injects an electron into the conduction band of the semiconductor. Positively charged dyes are then reduced by the iodide species I^- and the electrical circuit is completed by the reduction of I_3^- at the platinum counter electrode. Usually, Pt is used as the catalytic material and indium (or fluorine)-doped tin oxide (ITO or FTO) glass as the substrate for counter-electrode.

Although Pt exhibits excellent catalytic activity for tri-iodide reduction and good electric conductivity, it presents chemical instability with some electrolyte's solvents[3] and, consequently, a reduction of efficiency in the time.[4,5] Among the basic components of a DSSC system, the conductive glass substrates accounts indeed for approximately 50% of the total DSSC cost.[6] This is mainly attributable to the cost for the ITO (or FTO) deposition under high vacuum condition that is required to prepare the conductive glass plates. So, to further decrease the production costs and maintain acceptable cell efficiency in the time, both the platinum layer and conductive glass, should be replaced by cheaper materials implementable through easily reliable fabrication technologies.

Beside this, for the fabrication of dye solar cells on plastic substrates, indium tin oxide (ITO)-coated polymeric plates (mainly polyethylene naphthalate, PEN and polyethylene terephthalate, PET) are generally used.[7−9] But ITO's rigid inorganic crystal structure develops hairline fractures upon bending and detaches from the polymer substrate thus detracting to the overall electrical performance of the device. Consequently, developing an alternative counter-electrode capable to guarantee flexibility, lightness, high catalytic activity, low electrical resistance, and at the same time, low production cost is still an attractive and open issue.

With this aim, inexpensive carbonaceous materials such as graphite,[10,11] carbon black,[12] activated carbon,[13] hard carbon

Received: June 28, 2011
Accepted: August 26, 2011
Published: August 26, 2011

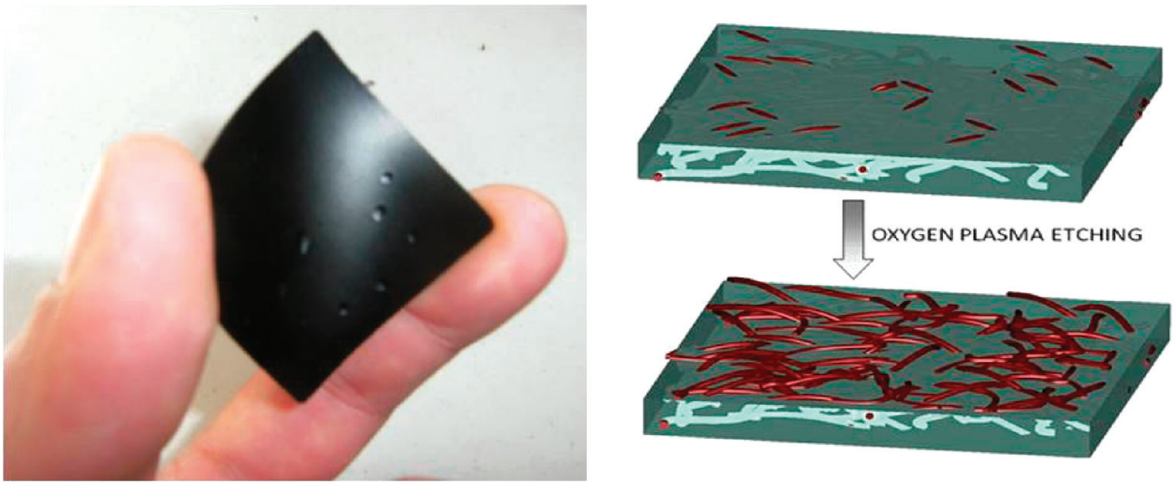

Figure 1. Real picture (left) of a CNT-based monolithic counter electrodes and a schematic representation (right) of etching treatment effect.

sphere,[14] mesoporous carbon,[15,16] and graphene[17−20] have been recently employed as catalytic films onto either conductive and not conductive substrates for making DSSC's counter-electrodes. Such carbonaceous materials are generally mixed with suitable binders and fillers to prepare electro-catalytic carbon-based paste or inks.

The best achievements, however, have been reported by means of a convenient utilization of carbon nanotube-based coatings (both single and multiwalled), because of their excellent catalytic properties and extremely high electrical conductivity (1×10^5 to 1×10^8 S m^{-1})[21] that are combined with large surface area and high chemical stability.[5,22] Several different counter electrodes have been so far realized by depositing specifically prepared CNTs-containing inks or sols onto FTO-coated glass,[22−25] onto metallic support[26] or flexible graphite.[13] As high as 10% values of solar energy conversion efficiency have been recently demonstrated with a vapor deposited film of aligned CNTs.[27] However, in all the previously published works, when CNTs have been implemented in the form of conductive cover layers onto bare glass or polymeric substrates (that is without FTO or ITO underlying coating), lower DSSC efficiency values and/or poor adhesion have been reported as major drawbacks.[28,29]

Starting from these remarks, we have been focused on the development of an engineered polypropylene/CNTs nanocomposite material with the purpose to develop suitable flexible and low cost plates to be effectively used as free-standing counter-electrodes in dye solar cells. Our 2-fold target was indeed to replace both platinum film and the conductive substrate, by exploiting the major chemical stability of the carbonaceous materials with respect to the I^-/I_3^- redox couple, as well as to realize an highly flexible counter electrode whose surface electric and catalytic properties result to be adequately preserved even when subjected to vigorous bending conditions. To the best of our knowledge, this paper constitutes to date the first report of a free-standing carbon−polymer composite plate that has been successfully used as counter-electrode in dye solar cells.

2. EXPERIMENTAL SECTION

Preparation of the Nanocomposite Plates. Multiwalled carbon nanotubes (MWCNTs) with 50−100 nm diameter, 10−20 μm length, and functionalized with carboxylic group (−COOH) (purchased from Cheap Tubes) have been dispersed in toluene and sonicated for 90 min to untie the entanglements. A polypropylene with number-average molecular weight of 190 000 Da was dissolved under reflux in toluene. The two solutions were then mixed together for 2 h and the solvent was finally removed in a vacuum at 60 °C for all night long. The resulting powder was then modeled by compression molding (temperature 210 °C, pressure 5 MPa for 10 min) into a thin plate with thickness of about 300 μm (Figure 1). Different nanocomposite (NC) plates have been prepared by varying the weight percentage of CNTs. In the following lines, the acronyms NC5, NC10, NC15, and NC20 will be referred to plates based on a CNT content of 5, 10, 15, and 20%, respectively.

Oxygen Plasma Etching. Top surface of the plates was etched by oxygen plasma with the aim to remove the polymer capping layer and allows CNTs to partially merge from the matrix. Plasma treatments were performed in a IONVAC inductively coupled plasma (ICP) reactor (PGF 600 RF HUTTER): the samples were placed into the chamber, followed by evacuation to 30 mTorr, O_2 gas was introduced at a flow rate of 20 sccm (standard cubic centimeter per minute), and the glow discharge was ignited at 150 W. The same treatment was executed on both sides of the plates so to make possible the electrical connection. In Figure 1, a schematic representation of our free-standing nanocomposite counter electrode before and after etching treatment.

Fabrication of Dye Solar Cells. FTO-coated glass samples have been bathed in a detergent solution with an ultrasonic bath for 15 min consequently been washed with water and ethanol. Then, a screen-printable paste containing 30 nm-sized TiO_2 colloids was prepared according to a procedure reported earlier[30] and deposited onto the conducting glass by screen-printing (screen characteristic: material, polyester; mesh count, 120 mesh/cm) through a 0.12 cm^2 large mask and dried at 160 °C for 6 min; this procedure was repeated several times in order to obtain 14 μm thick photoelectrodes. The film thickness and the dimensions of the active area were measured using KLA-TENCOR profilometer. The FTO-glass samples coated with the TiO_2 pastes were gradually heated under an air flow at 160 °C for 20 min, 325 °C for 5 min, at 375 °C for 5 min, at 450 °C for 15 min, and at 500 °C for 15 min. After being cooled to 80 °C, the TiO_2 electrodes were immersed into a solution 0.5 mM of bis(tetrabutylammonium)-cis-di(thiocyanato)-N, N′-bis (4 - carboxylato -4′ - carboxylic acid-2, 2 -bipyridine) ruthenium-(II) (N719) in a mixture of acetonitrile and tert-butyl alcohol (v/v, 1:1), and kept at room temperature for 14 h.

The solar cells were assembled by placing a nanocomposite plate (counter electrode) on the N719 dye-sensitized photoelectrode

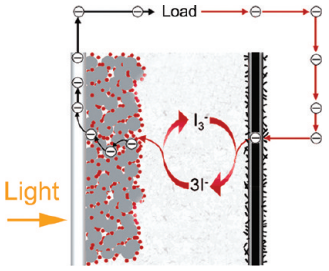

Figure 2. Schematic representation of a dye solar cell mounting a monolithic CNT-based nanocomposite counter electrode electrically contacted from its rear side.

(working electrode). The two electrodes were then further assembled into a sandwich type cell and sealed with an 120 μm thick Parafilm hot-melt gasket. The redox electrolyte was introduced into the space of interelectrodes through a hole predrilled on the photoelectrode. The holes were sealed up using Surlyn hot-melt film and a cover glass. The redox electrolyte used was 0.1 M LiI, 0.05 M I_2, 0.6 M 1-methyl-3-propylimidazolium iodide, and 0.5 M tert-butylpyridine in dried acetonitrile.

It has to be highlight that electrical connection to the counter-electrode has been realized on the back-side of the plate as clarified in the Figure 2.

Morphological and Electrochemical Characterization. SEM characterization of both bare and etched surfaces was performed with a RAITH-150 EBL instrument. Either electrical resistivity and photocurrent−voltage measurements were performed using a Keithley unit (Model 2400 Source Meter). Disk-shaped samples (5 mm in diameter and 260 μm in thickness) were prepared for testing the electrical properties. The DC conductivity was measured using the four-point probe method. A Newport AM 1.5 Solar Simulator (model 91160A equipped with a 300 W xenon Arc Lamp) served as a light source and its light intensity (or radiant power) was calibrated to 100 mW/cm^2 using a reference a Si solar cell. Cyclic Voltammetry (CV) and Electrochemical Impedance Spectroscopy (EIS) spectra have been measured by using an AUTOLAB PGSTAT 100 potentiostat operating in two-electrode mode. Frequency range 100 kHz to 10 mHz for dummy cells; AC voltage 10 mV. The frequency-dependent impedance was fitted by using the FRA-AUTOLAB software with the aim to obtain information on NC plates/electrolyte interface varying the plasma etching time and CNTs percentage into the matrix.

3. RESULTS AND DISCUSSION

As a consequence of the thermomechanically induced viscous motions of the polypropylene chains, surfaces of the plates prepared by hot-molding process did not present CNTs protruding from their top because they were totally covered by a thick polymeric capping layer.

To remove such an electrically insulating shell and allow catalytic carbonaceous fillers to merge on top of the surface, we carried out a series of properly setup reactive ion etching treatments with oxygen plasma. Tuning of the morphological features of the composite surface was possible by adjusting the parameters that regulate the plasma etching conditions: having evaluated different combinations of process parameters, we finally established the use of a fixed set of etching conditions (O_2 flow, 20 sccm; pressure, 30 mTorr; voltage, 620 V) and varied the exposure time from 5 to 120 min.

In Figure 3, we report a set of SEM images of NC5 plate surfaces that have been subjected to plasma etching with different exposure times as well as a picture of an untreated surface (Figure 3a) as reference. After a 5 min long exposure, CNTs started to outcrop (Figure 3b), but they were still almost completely embedded into the PP matrix. As result of the selective etching, a randomly textured surface was generated as a proof of the homogeneity in the CNTs dispersion. After longer plasma etching times−30 min (Figure 3c) and 60 min (Figure 3d), respectively−the formation of deeper interconnected channels became clearly detectable and CNTs filaments were finally unfolded from the PP matrix. It is then evident how this treatment increases the roughness and the superficial contact area of the nanocomposite because it allows us to remove the undesired polymeric shell and maximize the CNTs exposition.

The impact of the surface treatment on the electric resistance of the plate was evaluated by means of CV and EIS measurements, which were performed on test cells having an Pt/Electrolyte/NC sandwich configuration[31] and an active area of 0.2 cm^2. CV plots as obtained for a 5 wt % MWCNTs-based counter-electrode are reported in Figure 4a.

The effect of etching treatments is essentially 2-fold: it determines both a reduction of the activation voltage (right shift of the curves), that is the potential to be provided to allow an effective iodide reduction (as indicated by the first horizontal part of the voltammogram trace), and a substantial variation of slope in the second part of the graphic (the straight oblique part), thus indicating a faster reduction of the oxidized species. We can explain the first finding in terms of variation of both the bulk resistance of the nanocomposite R_{NC} and the charge transfer resistance at the interface $R_{ct(NC/El.)}$: they are in fact hugely reduced as an effect of the oxygen plasma treatment. The second finding depends instead on the effectiveness of the polymeric capping layer removal and on the extent of micro- and nanochannels thus generated: as expectable, as the superficial area of CNTs wetted by the electrolyte rises up, the electrolyte/NC interaction results to be improved and, correspondingly, the charge transfer resistance goes down.

A substantial minimization of the overall series resistance was obtained after a 30 min long plasma exposure. With longer treatment durations, a substantial saturation of the R_s value was observed, but the charge transfer resistance R_{ct} still exhibited a slight decrease; it is reasonable to suppose in fact that, after a 30 min long plasma treatment, not only the polymeric matrix, but even the protruding CNTs began to be subjected to the etching process.[32−34] This is known to induce the formation of oxygen superficial defects that can further beneficially affect the CNTs catalytic properties.[35]

So we verified that, in the case of NC5 plates, a 60 min long exposure was substantially sufficient to minimize the overall series resistance of the cell. This can be further confirmed by correlating the value of the cathodic peak voltage (V_{CP}) to the duration of plasma treatment as reported in Figure 4b: for exposure times longer than 60 min, V_{CP} shows the tendency to saturate toward a value of about −0.62 V.

In a DC condition analysis, the series resistance of the test cells can be evaluated as due to the following contributions

$$R_{Series} = (R_{NC} + R_{El.} + R_{Pt})_s + (R_{ct(NC/El.)} + R_{ct(El./Pt)})_{ct} + R_{diff(\Gamma_2)} = R_s + R_{ct} + R_{diff(\Gamma_2)} \quad (1)$$

where R_{NC} is the bulk resistance of the nanocomposite, $R_{El.}$ the electrolyte resistance, R_{Pt} the sheet resistance of the platinum, $R_{ct(NC/El.)}$ the charge transfer resistance between NC and

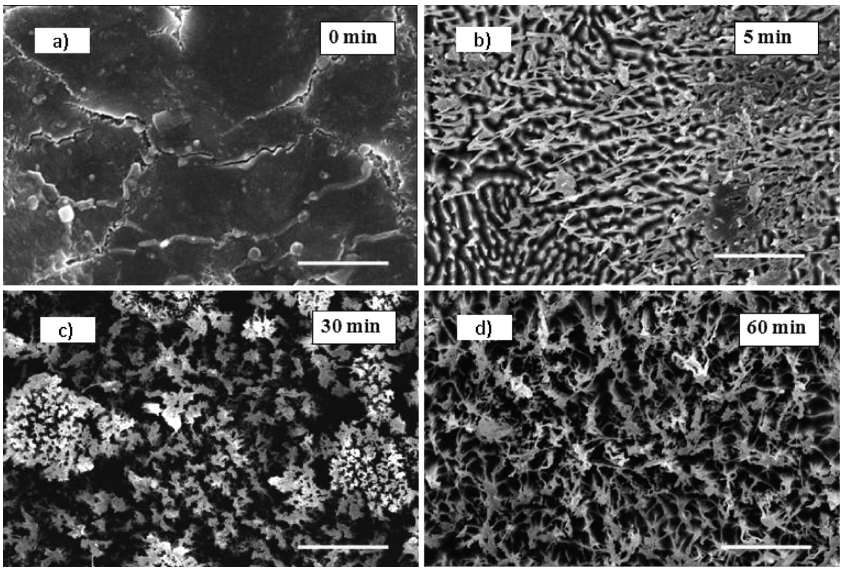

Figure 3. SEM images of the top surface of 5 wt % MWCNTs-based nanocomposite plates treated with oxygen plasma at different exposure times. Scale bar 1 μm.

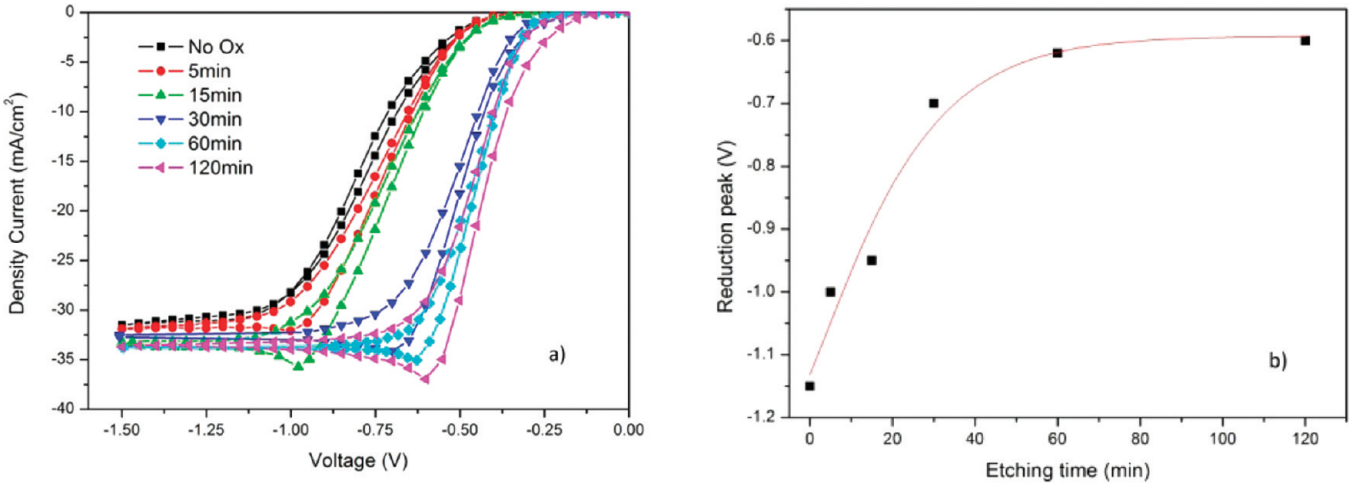

Figure 4. (a) Cyclic voltammetry plots of NC5-based counter-electrode treated with plasma oxygen at different exposure time; (b) trend of the cathodic peak voltage V_{CP} versus plasma exposure time.

electrolyte, $R_{ct(El./Pt)}$ the charge transfer resistance between electrolyte and platinum, and $R_{diff(\Gamma_2)}$ is the Nernst diffusion resistance within the electrolyte. The series resistance R_s is the sum of the bulk resistance of the nanocomposite (through its 260 μm thick cross section), the electrolyte resistance and the Pt sheet resistance.

In general, at low voltages the $R_{ct(NC/El.)}$ effect is predominant, whereas at higher voltages, the $R_{diff(\Gamma_2)}$ prevails.

Therefore, to quantitatively valuate the effect of the etching duration treatment on the different components of the series resistance of cell, we carried out an impedance spectroscopy analysis. In Figure 5 we report the Nyquist plots obtained from EIS measurements ranged from 100kHz and 10mHz at −0.5 V of NC5-based counter-electrodes treated with plasma oxygen at different exposure times.

The most meaningful parameter to characterize the NC/electrolyte interface is the charge transfer resistance, $R_{ct(NC/El)}$, that is the real part of the high-frequency arc.

As observable, only two semicircles are detectable in correspondence of that applied bias voltage: the first one (high frequencies) concerns either the Pt/electrolyte and NC/electrolyte interface: the frequency responses of CNTs-based plates and Pt-coated electrode result in fact to be not distinguishable in the Nyquist plot since they exhibit quite close values of the charge transfer coefficient; the second one (low frequencies) is referred to the contribute due to the Nernst diffusion impedance into the electrolyte. It is interesting to observe how increasing the etching time treatment the first arc decreases, whereas second increases. This is in perfect agreement with the CV curves: in fact, at −0.5 V, the tangents of the curves have different slope and this is recognizable into reduction of R_s and first arc; the beginning of the diffusional limit, for the samples more exposed to plasma, is revealed by the increase in the second arc.

Then, it has been revealed that as the etching time gets longer, the R_s and the size of the high-frequency arc decrease. Indirectly, the R_s give us information about the bulk resistance of the plate

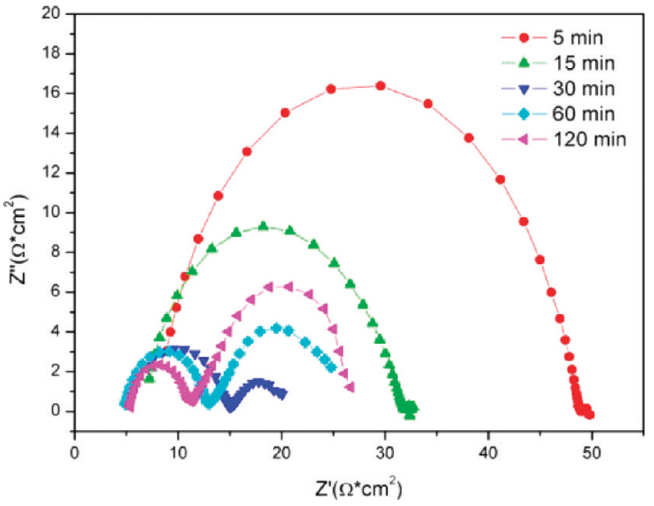

Figure 5. Nyquist plot obtained from EIS measurement at −0.5 V of NC5-based counter-electrode treated with plasma oxygen at different exposure times.

Table 1. Electrochemical Parameters of NC5 varying the etching time Exposition

etching time (min)	R_s (Ω*cm^2)	$R_{ct(NC/El)}$ (Ω*cm^2)	Y_0 (S)	n
5	8.78	37.85	2.4×10^{-6}	0.88
15	7.62	22.84	6.7×10^{-6}	0.84
30	5.24	8.87	2.2×10^{-5}	0.82
60	4.84	6.68	3.0×10^{-5}	0.87
120	5.02	5.25	2.7×10^{-5}	0.88

(eq 1). The R_s decreases up to 30 min of etching time treatment and, later, become stable: in fact from the initial condition, this parameter is reduced by one-third and stabilizes around 5 Ω*cm^2. The charge transfer resistance resulted reduced by almost 1 order of magnitude when the etching time passed from 5 to 120 min. Another important parameter is the constant phase element (CPE) given by admittance Y_0 and ideality factor "n". The behavior of this parameter is important because gives us a measure of the capacitive effect on the surface, that increases with higher exposition of catalytic part, and then of CNTs, to electrolyte. Even this parameter changes of 1 order of magnitude.

In Table 1, the extrapolated values of the most meaningful parameters are reported. To faithfully fit the experimental data, the equivalent circuit for a sandwich cell configuration detailed by Murakami and Grätzel was used.[31] Namely: the series resistance R_s, that has been calculated from intercept of the highest frequencies arc with real Z' axis; the charge transfer resistance at NC/electrolyte interface $R_{ct(NC/El)}$; the admittance Y_0 and the capacitor ideality's coefficient "n", which determine the value of the constant phase element (CPE).

In light of the above referred experimental concerns, it can be deduced that the etching treatment conditions dramatically affects the electrochemical properties of the NC/electrolyte as well as the value of the series resistance of the plate. Then, having studied and optimized the catalytic properties of the NC5 plate, through a 120 min oxygen plasma exposure, we tuned the CNTs concentration in the casting solution and then compared their electrochemical properties with those ones of a Pt coated ITO-glass counter-electrode as reference. Each plate was subjected to

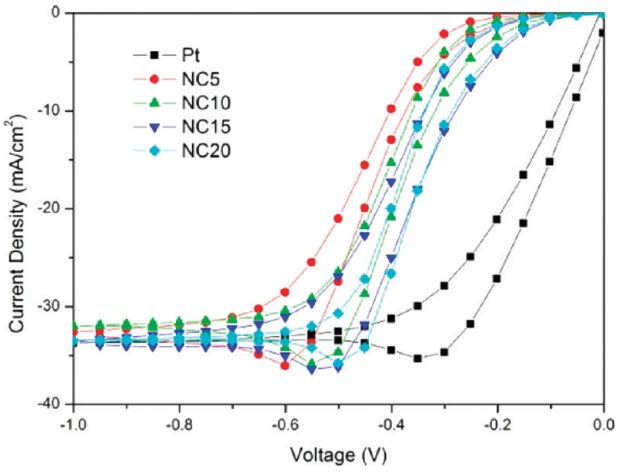

Figure 6. Cyclic voltammetry plots of NC plates containing different percentage of CNTs (from 5 to 20 wt %) compared with a reference Pt coating.

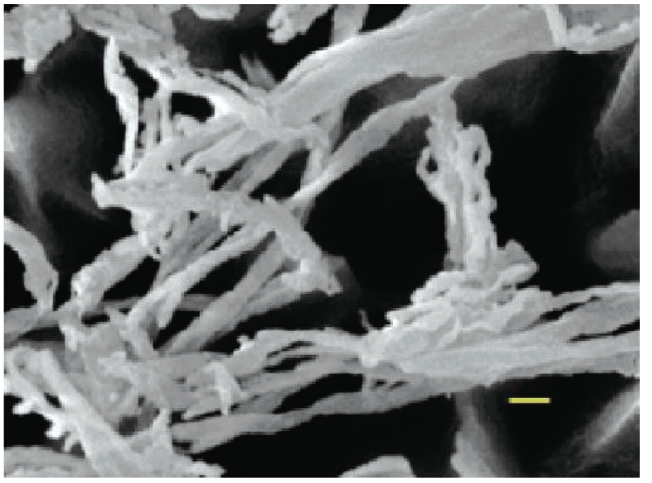

Figure 7. High-magnification SEM image of a NC20 surface exposed to a 60 min long plasma oxygen treatment. Scale bar: 100 nm.

a specific oxygen plasma treatment capable to minimize the electrochemical charge transfer resistance: 120 min for samples with 5 and 10 wt % of CNTs, 60 min for those with 15 and 20 wt %.

Figure 6 shows the CV plots obtained from test cells mounting respectively NC5, NC10, NC15 and NC20 etched plates. As a reference, the diagram obtained with a Pt/electrolyte/Pt reference cell is also reported. When CNTs content in the composite was increased, a significant reduction of the activation voltage as well as a right-shift of the cathodic peak voltage were detected, whereas the slope of the linear stretch of the curve results practically the same as in the case of Pt reference, thus indicating that the reduction rate of electrolyte by NC plates is comparable to that of platinum. But what we want to highlight is the different behavior of platinum and NC at interface with electrolyte: in fact, while platinum exhibited a perfectly ohmic behavior, our NC shows one nonlinear. It has been already demonstrated that, in spite of they are generally classified as p-type semiconductors, CNTs are capable to generate an ohmic interface when directly wetted by a conventional I^-/I_3^--based liquid electrolyte because

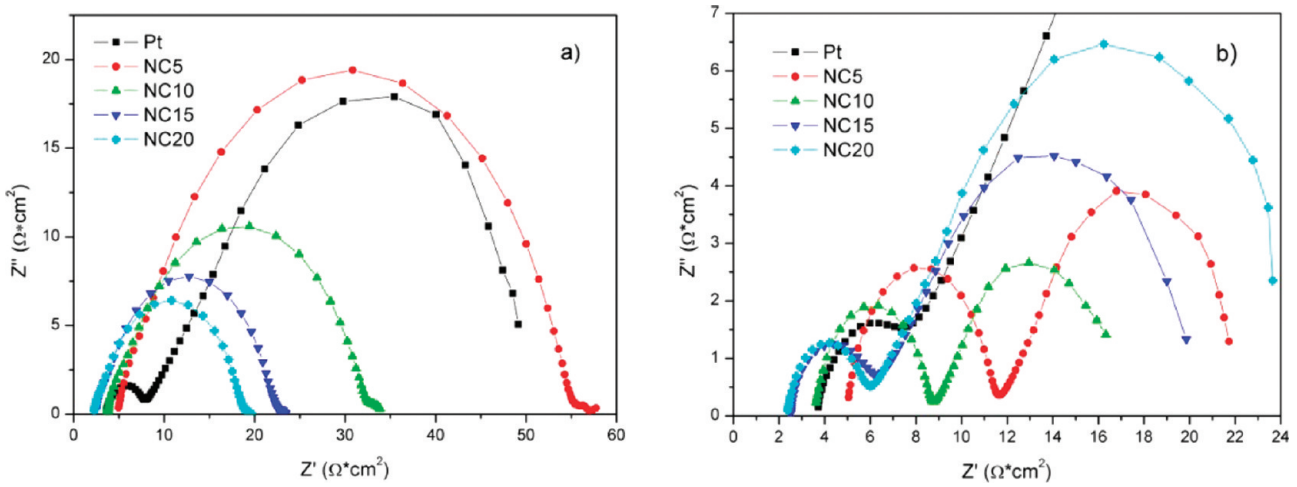

Figure 8. Nyquist plots of DSSCs implementing nanocomposite monolithic counter electrodes with different CNT contents. Measurements have been performed at two different bias voltage values: (a) −0.3 and (b) −0.5 V.

Table 2. Electrochemical Parameters of Pt and NC Counter Electrodes at −0.3 V and −0.5 V

	R_s (Ω*cm^2)	R_{ct} @ −0.3 V (Ω*cm^2)	R_{ct} @ −0.5 V (Ω*cm^2)
Pt	3.83	1.8	1.84
NC5	5.02	48.2	5.25
NC10	3.61	26.7	3.46
NC15	2.46	18.5	1.86
NC20	2.42	16.4	1.67

Table 3. Performances of DSC Mounting Pt and NC Plate Counter-Electrodes

CE	FF	V_{oc} (V)	J_{sc} (mA/cm^2)	η (%)
Pt reference	0.71	0.78	13.95	7.72
NC5	0.37	0.64	10.80	2.55
NC10	0.37	0.79	12.05	3.52
NC15	0.52	0.80	13.55	5.63
NC20	0.59	0.82	13.80	6.67

of their excellent conductivity.[36] Our NC plates revealed instead a nonlinear behavior that is associated to the presence of a potential barrier at the interface with electrolyte as attested by the almost horizontal slope of the curve at extremely low voltages. This behavior can be certainly ascribed to the persistence of a polymeric capping layer still surrounding a conspicuous part of the protruding CNTs surfaces after the etching process. In fact, even in the case of high CNTs concentration and after the etching process, a residual amount of polymer may led to a localized reduction of the total catalytic surface area wetted by the electrolyte. As a proof, in Figure 7, we report the SEM micrograph of an as obtained NC20 surface after a 60 min long plasma oxygen exposure that clearly shows the presence of polymeric tangles still grafted within the CNTs bundles.

The potential barrier, generated by the residual part of polymer, is overcome beyond a certain voltage. Then, to highlight the different behavior in the two regions, we carry out EIS analysis at −0.3 and −0.5 V on Pt/electrolyte/NCs and Pt/electrolyte/Pt cells.

From the fitting of the Nyquist plots at −0.3 V (see Figure 8a), is evident the R_{ct} depends by CNTs concentration: a sharp R_{ct} drop, from 48.2 to 16.4 Ω*cm^2, was detected as carbon nanotubes percentage increased, respectively from 5 to 20 wt %. However, even the higher concentration nanocomposite plate presents a Rct one order of magnitude higher than that of platinum. This affects the series resistance of the cell and then the fill factor.[37] At −0.5 V (see Figure 8b), the R_{ct} of all different concentration plates goes down almost 1 order of magnitude: so NC15/electrolyte interface shows practically the same value (1.86 Ω*cm^2) of the Pt/electrolyte interface (1.84 Ω*cm^2), and NC20 plate exhibited an even lower value (1.67 Ω*cm^2).

Finally, aside from their frequency response, NCs plate showed extremely low values of R_s: indeed, in the cases of NC15 and NC20 plates, these values resulted lower than Pt-based cell. It is certainly ascribable to the choice to adopt a backside electrical connection to test the MWCNTs/PP nanocomposite plates (as referred in the Experimental Section), but the low R_s values allow even to attest their good bulk electrical conductivity (eq1). Numerical values of R_s and R_{ct} at −0.3 and −0.5 V, respectively, are summarized in Table 2.

We finally implemented the above referred set of MWCNTs-based NC plates as monolithic counter electrodes (CE) in dye-sensitized solar cells. The values of efficiency (η%), fill factor (FF), open circuit voltage (V_{OC}), and short-circuit current density (J_{SC}) measured for these DSSCs are reported in Table 3, whereas the $J-V$ (current density−voltage) curves are shown in Figure 9. The same trend observed from the electrochemical characterization, was detected even from the analysis of the photovoltaic performances. DSSCs mounting NC5 and NC10 CEs produced relatively low photocurrent densities and inadequate fill factor; these effects are attributable either to their high charge transfer resistance, which is in turn related to the insufficient surface CNTs density exposed to the electrolyte, as well as to the high bulk resistance of the plates. NC15 and NC20 exhibited instead high photocurrent densities, comparable with the value of the reference Pt counter-electrode, and high open circuit voltages, but still lower fill factor. In view of a J_{SC} of 13.95 mA/cm^2 as well as a power-conversion efficiency of 7.72% produced by Pt-based CE, NC20-based CE rendered in fact a

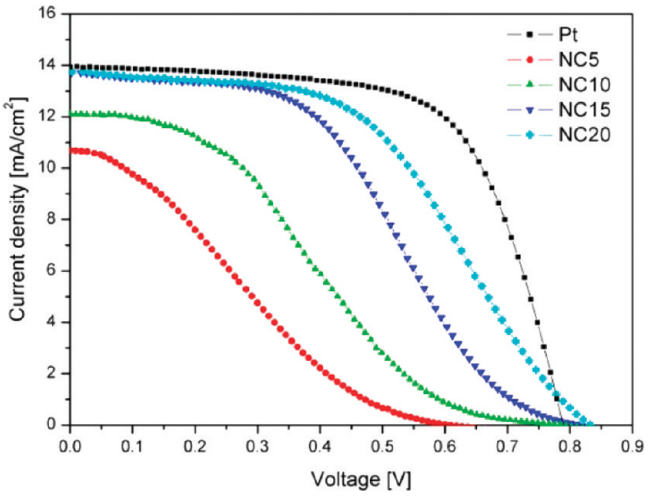

Figure 9. $J-V$ curves of DSSCs implementing nanocomposite monolithic counter electrodes with different CNT contents.

J_{SC} value of 13.80 mA/cm^2 and an η of 6.67% (Table 3). The lower η for the CNTs-based CEs is due to, as referred above, the presence of an energy barrier at the interface with electrolyte that turns into insufficient fill factor values. All the NCs-based cells exhibited in fact an S-like shaped $J-V$ curve that is intrinsically correlated to the nonlinear electrical behavior NC/electrolyte interface. As detected from the cyclic voltammetry analysis, the intensity of the energy barrier lies in the range between 0 and −0.3 V and its value strongly depends on the CNTs surface density. Correspondingly, it has to be highlighted that in the $J-V$ characteristics the load voltage corresponding to the inflection point shifted from 0.34 to 0.63 V as the CNTs raised from 5 to 20 wt %. In other terms, there is a direct relationship between the activation energy threshold revealed from the CV analysis and the position of the inflection point in the $J-V$ characteristics.

4. CONCLUSIONS

We successfully implemented a flexible MWCNTs-based polypropylene composite plate as effective monolithic counter-electrode for dye solar cells. A maximum photocurrent density of 13.8 mA/cm^2, as along with a solar conversion efficiency of 6.67%, has been obtained for a dye solar cell mounting an optimized counter-electrode, that is based on 20 wt % concentration of MCWNTs and has been subjected to a 60 min long plasma exposure. Both morphological and electrochemical analysis revealed that the oxygen plasma treatment constitutes an easy and effective method to selectively remove the excess polymer of this nanocomposite, allowing CNTs to properly protrude from the polymeric matrix.

It is worth remarking also that the proposed approach to the fabrication of CNT-based counter-electrode has the great potential to be low-cost and easily extendible on large production scales. The implementation of such a monolithic sheet of catalyst may represent an extremely valid solution to the problems related to the weak substrate adhesion strength referred to the coating-based approaches (especially in the case of plastic substrates) as well as those related to the extreme volatility of CNTs deposited by conventional spray-coating or inkjet printing techniques.

AUTHOR INFORMATION

Corresponding Author
*E-mail: michele.manca@iit.it.

ACKNOWLEDGMENT

This work has been partially supported by the National Network on Nanoscience Research — ItalNanoNet — Project code: RBPR05JH2P. We thank Sonia Carallo and Diego Mangiullo for their precious technical support and Alessandro Cannavale and Domenico Sergi for helpful discussions.

REFERENCES

(1) O'Regan, B.; Gratzel, M. *Nature* **1991**, *353*, 737–740.
(2) Tulloch, G. E. *J. Photochem. Photobiol., A* **2004**, *164*, 209–219.
(3) Olsen, E.; Hagen, G.; Eric Lindquist, S. *Sol. Energy Mater. Sol. Cells* **2000**, *63*, 267–273.
(4) Kay, A.; Grätzel, M. *Sol. Energy Mater. Sol. Cells* **1996**, *44*, 99–117.
(5) Koo, B.-K.; Lee, D.-Y.; Kim, H.-J.; Lee, W.-J.; Song, J.-S.; Kim, H.-J. *J. Electroceramics* **2006**, *17*, 79–82.
(6) Smestad, G.; Bignozzi, C.; Argazzi, R. *Sol. Energy Mater. Sol. Cells* **1994**, *32*, 259–272.
(7) Chen, L.; Tan, W.; Zhang, J.; Zhou, X.; Zhang, X.; Lin, Y. *Electrochim. Acta* **2010**, *55*, 3721–3726.
(8) Yin, X.; Xue, Z.; Liu, B. *J. Power Sources* **2009**, *196*, 2422–2426.
(9) Nemoto, J.; Sakata, M.; Hoshi, T.; Ueno, H.; Kaneko, M. *J. Electroanal. Chem.* **2007**, *599*, 23–30.
(10) Gagliardi, S.; Giorgi, L.; Giorgi, R.; Lisi, N.; Dikonimos Makris, T.; Salernitano, E.; Rufoloni, A. *Superlattices Microstruct.* **2009**, *46*, 205–208.
(11) Denaro, T.; Baglio, V.; Girolamo, M.; Antonucci, V.; Arico', A.; Matteucci, F.; Ornelas, R. *J. Appl. Electrochem.* **2009**, *39*, 2173–2179.
(12) Li, P.; Wu, J.; Lin, J.; Huang, M.; Huang, Y.; Li, Q. *Solar Energy* **2009**, *83*, 845–849.
(13) Chen, J.; Li, K.; Luo, Y.; Guo, X.; Li, D.; Deng, M.; Huang, S.; Meng, Q. *Carbon* **2009**, *47*, 2704–2708.
(14) Huang, Z.; Liu, X.; Li, K.; Li, D.; Luo, Y.; Li, H.; Song, W.; Chen, L.; Meng, Q. *Electrochem. Commun.* **2007**, *9*, 596–598.
(15) Wang, G.; Wang, L.; Xing, W.; Zhuo, S. *Mater. Chem. Phys.* **2010**, *123*, 690–694.
(16) Ramasamy, E.; Lee, J. *Carbon* **2010**, *48*, 3715–3720.
(17) Hong, W.; Xu, Y.; Lu, G.; Li, C.; Shi, G. *Electrochem. Commun.* **2008**, *10*, 1555–1558.
(18) Wan, L.; Wang, S.; Wang, X.; Dong, B.; Xu, Z.; Zhang, X.; Yang, B.; Peng, S.; Wang, J.; Xu, C. *Solid State Sci.* **2011**, in press.
(19) Roy-Mayhew, J. D.; Bozym, D. J.; Punckt, C.; Aksay, I. A. *ACS Nano* **2010**, *4*, 6203–6211.
(20) Choi, H.; Kim, H.; Hwang, S.; Choi, W.; Jeon, M. *Sol. Energy Mater. Sol. Cells* **2011**, *95*, 323–325.
(21) McEuen, P. L.; Fuhrer, M. S.; Hongkun, P. *IEEE Trans. Nanotechnol.* **2002**, *1*, 78–85.
(22) Lee, W. J.; Ramasamy, E.; Lee, D. Y.; Song, J. S. *ACS Appl. Mater. Interfaces* **2009**, *1*, 1145–1149.
(23) Xiaoguang, M. *Nanotechnology* **2010**, *21*, 395202.
(24) Ramasamy, E.; Lee, W. J.; Lee, D. Y.; Song, J. S. *Electrochem. Commun.* **2008**, *10*, 1087–1089.
(25) Choi, H. J.; Shin, J. E.; Lee, G.-W.; Park, N.-G.; Kim, K.; Hong, S. C. *Curr. Appl. Phys.* **2010**, *10*, S165–S167.
(26) Lee, K.-M.; Chiu, W.-H.; Wei, H.-Y.; Hu, C.-W.; Suryanarayanan, V.; Hsieh, W.-F.; Ho, K.-C. *Thin Solid Films* **2010**, *518*, 1716–1721.
(27) Nam, J. G.; Park, Y. J.; Kim, B. S.; Lee, J. S. *Scr. Mater.* **2010**, *62*, 148–150.
(28) Suzuki, K.; Yamaguchi, M.; Kumagai, M.; Yanagida, S. *Chem. Lett.* **2003**, *32*, 28–29.

(29) Moon, J. S.; Park, J. H.; Lee, T. Y.; Kim, Y. W.; Yoo, J. B.; Park, C. Y.; Kim, J. M.; Jin, K. W. *Diamond Relat. Mater.* **2005**, *14*, 1882–1887.
(30) De Marco, L.; Manca, M.; Giannuzzi, R.; Malara, F.; Melcarne, G.; Ciccarella, G.; Zama, I.; Cingolani, R.; Gigli, G. *J. Phys. Chem. C* **2010**, *114*, 4228–4236.
(31) Murakami, T. N.; Grätzel, M. *Inorg. Chim. Acta* **2008**, *361*, 572–580.
(32) Huang, S.; Dai, L. *J. Phys. Chem. B* **2002**, *106*, 3543–3545.
(33) Mawhinney, D. B.; Naumenko, V.; Kuznetsova, A.; Yates, J. T.; Liu, J.; Smalley, R. E. *J. Am. Chem. Soc.* **2000**, *122*, 2383–2384.
(34) Liu, Y.; Liu, L.; Liu, P.; Sheng, L.; Fan, S. *Diamond Relat. Mater.* **2004**, *13*, 1609–1613.
(35) Trancik, J. E.; Barton, S. C.; Hone, J. *Nano Lett.* **2008**, *8*, 982–987.
(36) Chou, A.; Bocking, T.; Singh, N. K.; Gooding, J. J. *Chem. Commun.* **2005**, 842–844.
(37) Radziemska, E. *Energy Convers. Manage.* **2005**, *46*, 1485–1494.